Heliyon 9 (2023) e21064

Contents lists available at ScienceDirect

Heliyon

journal homepage: www.cell.com/heliyon

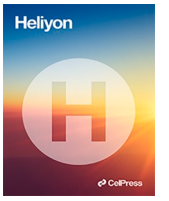

Traditional Banxia Xiexin decoction inhibits invasion, metastasis, and epithelial mesenchymal transition in gastric cancer by reducing lncRNA TUC338 expression

Xiaojun Dai [a,b,f,1], Yanwei Yu [f,1], Chen Zou [f,1], Bo Pan [f], Haibo Wang [f], Shanshan Wang [a], Xiaojuan Wang [f], Chenghai Wang [c,***], Dongmei Liu [d,e,**], Yanqing Liu [a,f,*]

[a] *Clinical College of Traditional Chinese Medicine, Yangzhou University, 577 Wenchang Middle Road, Yangzhou, 225002, China*
[b] *Traditional Chinese Medicine Hospital of Yangzhou, 577 Wenchang Middle Road, Yangzhou, 225002, China*
[c] *Department of Pathology, The Affiliated Hospital of Yangzhou University, Yangzhou University, 368 Hanjiang Middle Road, Yangzhou, 225009, China*
[d] *College of Chemistry and Chemical Engineering, Yangzhou University, 180 Siwangting Road, Yangzhou, 225002, China*
[e] *Jianghai Polytechnic College, 5 Yangzijiang South Road, Yangzhou, 225002, China*
[f] *Medical School, Yangzhou University, 136 Jiangyang Middle Road, Yangzhou, 225001, China*

ARTICLE INFO

Keywords:
Banxia Xiexin decoction
TCM
Gastric cancer
Knockdown LncRNA TUC338
Epithelial mesenchymal transition
Migration and invasion

ABSTRACT

Background: Banxia Xiexin decoction (BXD) is a classic traditional Chinese medicine (TCM) formula clinically used to treat chronic gastritis, gastric ulcers, gastric cancer, and many other gastrointestinal diseases. Long noncoding RNAs (lncRNAs) have been shown to play an important role in maintaining the malignant phenotype of tumors. However, no relevant studies have shown whether Banxia Xiexin decoction regulates and controls lncRNA TUC338, and the effect of TUC338 on the regulation of gastric cancer invasion and metastasis remains unclear.

Purpose: To investigate the ability of the traditional Chinese medicine (TCM) Banxia Xiexin decoction (BXD) to inhibit the migration and invasion of human gastric cancer AGS cells by regulating the long noncoding RNA (lncRNA) TUC338.

Methods: UHPLC–MS/MS was used to analyze the chemical components of BXD. MTT was performed to determine the effects of BXD on the proliferation of AGS cells. qRT–PCR was used to determine the expression of lncRNA TUC338 in gastric cancer tissues, paracarcinoma tissues, AGS human gastric cancer cells and GES-1 normal gastric mucosa cells and to evaluate the effects of BXD on the expression of lncRNA TUC338 in AGS cells. Lentiviral transfection was used to establish human gastric cancer AGS cells with knocked down lncRNA TUC338 expression. The effects of lncRNA TUC338 knockdown on the migration and invasion of AGS cells were observed by a scratch assay and Transwell migration assay, respectively. Western blotting was performed to analyze the effects of lncRNA TUC338 knockdown on epithelial-to-mesenchymal transition (EMT)

* Corresponding author. Clinical College of Traditional Chinese Medicine, Yangzhou University, 577 Wenchang Middle Road, Yangzhou, 225002, China.
** Corresponding author. College of Chemistry and Chemical Engineering, Yangzhou University, 180 Siwangting Road, Yangzhou, 225002, China.
*** Corresponding author. Department of Pathology, The Affiliated Hospital of Yangzhou University, Yangzhou University, 368 Hanjiang Middle Road, Yangzhou, 225009, China.
E-mail addresses: chwang@yzu.edu.cn (C. Wang), ldm2319@126.com (D. Liu), liuyq@yzu.edu.cn (Y. Liu).
[1] These authors contributed equitably to the work.

https://doi.org/10.1016/j.heliyon.2023.e21064
Received 13 January 2023; Received in revised form 8 October 2023; Accepted 13 October 2023
Available online 20 October 2023

in AGS cells. We performed quality control on three batches of BXD. We used UHPLC−MS/MS to control the quality of three random batches of BXD used throughout the study.
Results: Ninety-five chemical components were identified from the water extract of BXD, some of which have anticancer effects. The expression of TUC.338 in gastric cancer tissues was higher than that in para-carcinoma tissues. BXD inhibited the invasion and migration of gastric cancer cells by inhibiting the expression of lncRNA TUC338, which reduced EMT. After knockdown of lncRNA TUC338, the migration and invasion of AGS cells were reduced; the expression of the EMT-related protein E-cadherin was increased, and the expression of N-cadherin and vimentin was reduced.
Conclusions: The present results suggest that BXD has potential as an effective treatment for gastric cancer through the inhibition of lncRNA TUC338 expression.

1. Introduction

According to statistics, the annual number of gastric cancer cases in the world reached 1.089 million in 2020, ranking fifth among all malignant tumors. That same year, there were 769,000 deaths from stomach cancer, the fourth highest among all cancer types. The number of new global cases is expected to increase by 62 % to 1.77 million by 2040. In addition, nearly two-thirds of stomach cancer diagnoses in 2020 were in East and Southeast Asia [1,2], with China accounting for approximately 44 % of the global incidence, resulting in an enormous economic and public health burden. It is worth noting that the cure rate of early gastric cancer can reach 90 %, but the 5-year overall survival rate (OS) of advanced patients is less than 38 % [3], suggesting that metastasis is an important prognostic factor. Treating only the primary lesion of gastric cancer cannot achieve a desired therapeutic effect. Effective treatment of gastric cancer requires targeting cell migration and invasion to reduce metastasis. Therefore, it is urgent to develop drugs that can inhibit the metastasis of gastric cancer to improve the survival rate of patients.

The process of cancer metastasis is very complex and involves many aspects, among which epithelial mesenchymal transformation (EMT) is the key link in tumor metastasis. EMT is a biological process in which epithelial cells lose polarity and transform into mesenchymal cells with the ability to move freely [4]. The expression or function of epithelial genes is lost during the transition process, and phenotypes such as the expression level of genes that define mesenchymal cells are increased [5]. EMT leads to degeneration of the adhesion structure between tumor cells, increases invasiveness, leads to tumor metastasis, and increases the difficulty of treatment [6].

Long noncoding RNA (lncRNA), without a coding function, is greater than 200 nt in length, located in the nucleus or cytoplasm of the cell, and usually replicated by RNA polymerase II [7]. Due to the lack of an open reading frame (ORF), lncRNAs cannot encode proteins. Therefore, lncRNAs were initially considered “junk genes” or “genomic dark matter”. However, with in-depth research in recent years, it has been found that lncRNAs are widely involved in various physiological and pathological processes of organisms by regulating gene expression at the pretranscriptional, transcriptional and posttranscriptional levels [8–11]. Notably, there is increasing evidence that lncRNAs can regulate EMT by regulating EMT markers or transcription factors [12–14]. TUC338, as a newly discovered long noncoding RNA (lncRNA) in human tumors, is considered to be an oncogene. LncRNA TUC338 is overexpressed in bladder cancer [15], esophageal cancer [16], prostate cancer [17], and colorectal cancer [18] and regulates the EMT process. Our group previously found that both colorectal cancer tissues and cell lines showed a considerable upregulation of TUC338, and this upregulation was linked to lymph node metastasis [18]. SW480 and HCT116 colorectal cancer cell line migration and invasion were markedly reduced after TUC338 was knocked down using siRNA [18].

Banxia Xiexin decoction is a classic Chinese prescription created by Zhang Zhongjing that has been used clinically for 1800 years. BXD uses *Pinellia ternata* (Thunb.) Makino as the main herb, in addition to *Scutellaria baicalensis* Georgi, *Panax ginseng* C.A.Mey. and *Ziziphus jujuba* Mill, and *Zingiber officinale* Roscoe. In ancient times, BXD was often used to treat upset stomach. At present, Banxia Xiexin decoction contains brass, alkaloids and saponins and has a wide range of pharmacological effects against gastrointestinal diseases, including protecting the gastrointestinal mucosa, improving gastrointestinal diseases, regulating human endocrine metabolism, regulating neurotransmitters, and improving mood [19]. Modern studies have shown that Banxia Xiexin decoction has therapeutic effects on ulcerative colitis [20], gastritis [21], digestive tract tumors [22,23], irritable bowel syndrome [19] and other digestive tract diseases. Notably, existing studies have shown that Banxia Xiexin decoction can regulate the Wnt/β-catenin pathway to inhibit the proliferation and invasion of gastric cancer cells and induce apoptosis [24]. In another study, Banxia Xiexin decoction increased the sensitivity of GC cells to chemotherapy drugs and inhibited the proliferation of drug-resistant cells by inhibiting the expression of MGMT and PD-L1 [25].

However, no studies have shown whether TUC338 expression of lncRNAs can promote the invasion and migration of gastric cancer cells, nor is it clear whether Banxia Xiexin decoction can inhibit tumor invasion and migration by regulating TUC338 expression. Therefore, in the present study, the effects of BXD on cell migration, invasion, EMT and TUC338 expression in AGS gastric cancer cells were determined.

Table 1
Sequences of primers used in qRT-PCR.

Name	Forward primer (5′-3′)	Reversed primer (5′-3′)
TUC.338	5′-GTGACAAGGTGCCGGAT-3′	5′-CCAGGTCAGGGTTGAGG-3′
E-cadherin	5′-GGATAACCAGAATAAAGACCAAGTG-3′	5′-CCGAAGAAACAGCAAGCAG-3′
N-Cadherin	5′-GGACCATCACTCGGCTT-3′	5′-GCAAACCTTCACACGCA-3′
vimentin	5′-GAAGAGAACTTTGCCGTTG-3′	5′-GAAGGTGACGAGCCATTT-3′
GAPDH	GGTGAAGGTCGGTGTGAACG	CTCGCTGGAAGATGGTG

2. Materials

2.1. Cell culture

The human gastric cancer cell lines AGS and GES-1 were purchased from the Shanghai Cell Bank of the Chinese Academy of Sciences. Approval for this study was granted by the Institute of Research Medical Ethics Committee of the Affiliated Clinical College of Traditional Chinese Medicine, Yangzhou University (No. 2018–010, Yangzhou, China).

2.2. Drug preparation

BXD was prepared according to the components and proportions as follows (Pharmacopoeia of the People's Republic of China. 2020): *Pinellia ternata* (Thunb.) Makino 12 g, *Zingiber officinale* Roscoe 9 g, *Scutellaria baicalensis* Georgi 9 g, *Coptis chinensis* Franch. 3 g, *Panax ginseng* C.A.Mey. 9 g, *Ziziphus jujuba* Mill. 12 g, and *Glycyrrhiza uralensis* Fisch. 9 g (http://www.theplantlist.org/). All herbs were purchased from Affiliated Clinical College of Traditional Chinese Medicine, Yangzhou University. The decoction was prepared as follows: the herbs were soaked for 30 min, decocted twice for 30 min each, filtered through a double-layered gauze to remove the residue, evaporated in a water bath at 100 °C, resulting in an aqueous decoction containing 1 g of raw drug per mL, and then autoclaved and stored at 4 °C. 5-Fluorouracil (5-FU) was obtained from Shanghai Xudong Haipu Pharmaceutical Co., Ltd. (Shanghai, China).

2.3. Main reagents

The main reagents used in the present study were as follows: RPMI 1640 culture medium (HyClone, Logan, Utah, USA, cat# SH30809.01); fetal bovine serum (GIBCO, Grand Island, New York, USA, cat# 10099–141); MTT powder (Sigma, St. Louis, MO, USA, cat# M2128); trypsin-EDTA solution, penicillin–streptomycin mixture, puromycin, BCA quantitative kit, RIPA lysis solution (Beyotime Biotechnology Co., Ltd., Shanghai, China, cat# C0201, C0222, ST551, P0012S, P0013C, respectively); PVDF membrane (Millipore, BOSTON, MA, USA, cat# IPVH00010); antibodies specific for N-cadherin, E-cadherin, and vimentin (Thermo, Waltham, MA, USA, cat# 33–3900, 13-3249-82, MA5-16409, respectively); and Transwell (BD, Franklin, NJ, USA, cat# 353093).

3. Methods

3.1. UHPLC–MS/MS analysis

The components of BXD were examined using coupled ultrahigh-performance liquid chromatography-tandem mass spectrometry (UHPLC–MS/MS, Q Exactive Plus, United States). The BXD aqueous extract was separated using an ACQUITY UPLC HSS T3 column (2.1 × 100 mm, 1.8 μm). The injection had a 10 μL volume.

Aqueous acetonitrile (0.1 %) and formic acid made up the mobile phase. In this framework, chromatographic separation was carried out at 35 °C. The flow rate of gradient elution was 0.3 mL/min. Full MS-ddMS2 detection mode was used, the scanning range was *m/z* 100–1200, and the positive and negative ions were scanned in turn.

3.2. Cell culture

A sterile incubator with 5 % CO2 and a constant temperature of 37 °C was used to culture the cells in RPMI 1640 with 10 % fetal bovine serum. The status of the cells was observed daily, and the medium was changed appropriately. Trypsin was used to separate cells during the logarithmic growth phase so that they could be used in later research.

3.3. Cytostatic assay (MTT)

AGS cells were evenly infused onto 96-well plates (5×10^4 per well) while they were in the logarithmic growth phase. After the cells were incubated until they were attached, various concentrations of BXD solution (0.50, 1.00, 1.50, 2.00, 2.50 and 3.00 mg/mL) were added to each well (100 μL/well), with 5 replicate wells set for each concentration. All plates were incubated for 48 h, followed by adding 5 % MTT (20 μL/well) to react for 4 h. The supernatant was discarded. To dissolve the crystals, 150 μL of DMSO was added to

each well, and the plates were agitated for 10 min. The OD value was measured at 490 nm with an enzyme marker. The cell growth inhibition rate = (1 - OD value of drug group/OD value of the control group) × 100 %. The mean inhibitory concentration (IC50) was calculated using the linear equation (y = mx + b) using GraphPad Prism version 8.0 software.

3.4. Real-time fluorescence quantitative PCR (qRT–PCR)

Total RNA was extracted from human stomach cancer and paracarcinoma tissue samples. cDNA was synthesized by reverse transcription. Lentivirus was used to transfect AGS cells with AGS/TUC338 or empty vector AGS/TUC338-ctrl. The expression level of the TUC338 gene was determined by qRT–PCR using the SYBR GREEN method, including before and after BXD treatment. The primers used for the PCR are shown in Table 1. The volume of the total PCR system was 10 μL. The predenaturing conditions were as follows: 95 °C for 30 s, 1 cycle; 95 °C for 5 s; and 60 °C for 31 s, 40 cycles.

3.5. Construction of AGS cells with knockdown of lncRNA TUC338 expression

AGS cells in the logarithmic phase were seeded into 24-well plates. When the cells reached 60%–80 % confluence, the cells were washed 3 times with phosphate buffered saline (PBS), and 2 mL of serum-free RPMI-1640 medium was added to each well. Polybrene (20 μL) (infection sensitizer) was added to each well of the plate, followed by the addition of 2 μL of Lv-TUC338 or Lv-TUC338-ctrl. The plate was placed on a shaker to mix the reagents well and incubated for 16–20 h at 37 °C. After the virus-containing medium was removed, complete medium was added for 1–2 d. Then, complete medium containing 4 μg/mL puromycin (puromycin) was added for 1–2 d.

3.6. Cell migration assay (cell-scratch assay)

A 6-well plate was seeded with logarithmic phase human gastric cancer AGS cells (5×10^4). After the cells adhered, a thin scratch wound 2 mm wide was made in the middle of the well and washed twice with PBS. An untreated control group (wild-type AGS cells group), BXD group (0.50, 1.00, and 1.50 mg/mL), and a positive-control group (5-FU, 2 mg/mL) were set up. After 24 h of incubation, the width of the wound was observed under an inverted microscope and photographed. The rate of wound healing was also compared in AGS/TUC338-siRNA cells and AGS/TUC338-siRNA-ctrl cells.

3.7. Cell migration and invasion assays (Transwell assay)

Control AGS cells, no drug added, cells to be treated with BXD (0.50, 1.00, and 1.50 mg/mL), and cells to be treated with 5-FU (2 mg/mL) were seeded in the Transwell upper chamber (1×10^5) of Transwell plates. Five hundred microliters of RPMI with 10 % FBS was placed in the bottom chamber. Bubbles between the upper and lower layers were removed. After 12 h of incubation, the Transwell was removed and washed gently with PBS twice. The cells on the surface of the upper chamber membrane were wiped with cotton swabs, fixed in methanol for 30 min, stained with crystal violet for 20 min, and washed with PBS 3 times. The number of cells penetrating the membrane was examined under an inverted microscope and photographed for analysis. AGS/TUC338-siRNA cells and AGS/TUC338-siRNA-ctrl cells were also assayed for invasion capability in the Transwell assay.

3.8. Western blotting

AGS/TUC338-siRNA and AGS/TUC338-siRNA-ctrl cells were cultured to the logarithmic phase and seeded in 6-well plates (5×10^4). After 24 h of culture, the cells were washed twice with PBS. Total cellular protein was extracted, and the concentration was determined with the BCA method. After SDS–PAGE electrophoresis, the proteins were transferred to a PVDF membrane for 90 min, followed by blocking with TBST containing 5 % skim milk powder for 2 h at 4 °C. At 4 °C, a primary antibody (concentration 1:1000) was added and incubated overnight. The membrane was rinsed 3 times with TBST, and a secondary antibody (concentration 1:2000) was added and incubated for 2 h at room temperature. Emitter coupled logic (ECL) luminescence was performed to generate images for data analysis.

3.9. Statistical methods

Statistical analysis was performed with SPSS 23.0 statistical software. Differences between two groups were determined by two-tailed Student's *t*-test. Differences between three (or more) groups were analyzed using ANOVA. Significance was designated as follows: *, $p < 0.05$; **, $p < 0.01$; ***, $p < 0.001$. All experiments were repeated at least three times.

4. Results

4.1. Chemical components of BXD by UHPLC–MS/MS analysis

A total of 95 chemical components were identified from the water extract of BXD. The main components with OB ≥ 30 % and DL ≥ 0.18 include palmatine chloride (12.681 %; OB 64.6 %, DL 0.65), berberine (11.33 %; OB 36.86 %, DL 0.78), baicalin (10.95 %; OB

Table 2
Identification of the chemical components of BXD by UHPLC-MS/MS.

Name	Formula	Mass Deviation (ppm)	Molecular Weight (Da)	RT (min)	relative amount (%)
Palmatine chloride	C21H22ClNO4	1.44	351.14714	24.64	12.681
Berberine	C20H17 N O4	0.86	335.11604	24.923	11.330
Baicalin	C21H18 O11	0.6	446.08518	23.935	10.950
Sucrose	C12H22 O11	0.35	342.11633	1.651	10.126
Wogonoside	C22H20 O11	0.77	460.10092	25.825	10.066
Jatrorrhizine	C20H19 N O4	0.33	337.13152	23.289	5.949
2-Pyrrolidinecarboxylic acid	C5 H9 N O2	1.44	115.06349	1.646	4.531
Oroxylin A-7-O-β-D-glucuronide	C22H20 O11	0.8	460.10093	25.252	4.061
(+)-Magnoflorine	C20H23 N O4	0.97	341.16304	20.162	3.087
Glycyrrhizic acid	C42H62 O16	0.7	822.40436	30.077	2.804
Liquiritigenin	C15H12 O4	1.44	256.07626	23.556	2.621
Citric acid	C6 H8 O7	0.8	192.02716	3.323	2.317
Berberrubine	C19H15 N O4	1.16	321.10048	22.216	1.817
18 β-Glycyrrhetintic Acid	C30H46 O4	0.37	470.33978	30.06	1.769
Trigonelline HCl	C7 H7 N O2	1.83	137.04793	1.65	1.673
Baicalein	C15H10 O5	−1.61	270.05239	23.936	1.474
Liquiritin	C21H22 O9	1.05	418.12682	21.703	1.439
Stachyose	C24H42 O21	0.93	666.22248	1.663	1.417
Liguiritigenin-7-O-β-d-apiosyl-4′-O-β-D-glucoside	C26H30 O13	0.92	550.16915	21.524	1.208
Isoliquiritigenin	C15H12 O4	0.5	256.07369	21.517	0.756
Wogonin	C16H12 O5	−1.1	284.06816	25.826	0.592
Manninotriose	C18H32 O16	1.27	504.16968	1.659	0.584
Ginsenoside Rg1	C42H72 O14	1.44	846.49824	23.773	0.533
L-Glutamic acid	C5 H9 N O4	1.01	147.05331	1.504	0.496
Diammonium glycyrrhizinate	C42H62 O16	0.52	822.40421	31.035	0.444
5-Hydroxymethylfurfural	C6 H6 O3	1.6	126.0319	1.653	0.418
Oroxylin A	C16H12 O5	−1.12	284.06815	25.258	0.282
Demethyleneberberine	C19H17 N O4	0.14	323.1158	22.212	0.272
Glabrolide	C30H44 O4	1.56	468.32469	27.394	0.248
Ginsenoside Re	C48H82 O18	0.52	946.55061	23.738	0.213
Ononin	C22H22 O9	0.52	430.1266	23.924	0.207
Oxyberberine	C20H17 N O5	1.39	351.11116	22.494	0.177
Sophocarpine	C15H22 N2 O	1.75	246.17364	16.731	0.169
Formononetin	C16H12 O4	0.9	268.0738	29.568	0.168
Lupenone	C30H48 O	1.05	424.37096	27.689	0.149
Oxysophocarpine	C15H22 N2 O2	1.21	262.16844	17.051	0.142
Nicotinamide	C6 H6 N2 O	1.26	122.04817	3.153	0.137
Isoliquiritin	C21H22 O9	0.79	418.12671	23.996	0.132
Oroxin A	C21H20 O10	0.69	432.10594	23.921	0.128
Dehydroglaucine	C21H23 N O4	1.2	353.16313	22.558	0.128
Scutellarin	C21H18 O12	1.36	462.08045	21.929	0.119
Ferulic acid	C10H10 O4	1.58	194.05822	19.233	0.119
Ginsenoside Rf	C42H72 O14	1.17	800.49314	26.95	0.118
Taxifolin	C15H12 O7	0.93	304.05859	20.873	0.091
Ammothamnine	C15H24 N2 O2	1.68	264.18422	17.949	0.084
Quillaic acid	C30H46 O5	1.47	486.33524	28.912	0.083
Licochalcone B	C16H14 O5	0.39	286.08424	24.774	0.079
Tectorigenin	C16H12 O6	−0.21	300.06333	24.929	0.078
Luteolin	C15H10 O6	0.46	286.04787	23.859	0.077
Nicotinic acid	C6 H5 N O2	1.44	123.03221	2.772	0.076
Icaritin	C21H20 O6	1	368.12636	33.135	0.074
Puerarin	C21H20 O9	1.47	416.11135	22.718	0.074
Schaftoside	C26H28 O14	1.49	564.14875	20.47	0.070
Morin	C15H10 O7	0.95	302.04294	22.181	0.066
Retrochalcone	C16H14 O4	0.83	270.08943	27.354	0.065
Jaceosidin	C17H14 O7	0.92	330.07426	28.179	0.060
Ginsenoside Rc	C53H90 O22	0.51	1078.59292	28.178	0.058
Oxoglaucine	C20H17 N O5	0.6	351.11088	24.348	0.058
Isoacteoside	C29H36 O15	1.45	624.20633	22.122	0.057
Chrysin	C15H10 O4	−1.69	254.05748	25.331	0.055
Ginsenoside Rb1	C54H92 O23	1.44	2217.20645	27.682	0.049
Tectoridin	C22H22 O11	1.06	462.1167	24.899	0.049
Lysionotin	C18H16 O7	1.14	344.09	33.497	0.048
Azelaic acid	C9 H16 O4	1.16	188.10508	23.14	0.046
Gypenoside XVII	C48H82 O18	1.02	946.55109	29.735	0.044
Naringenin	C15H12 O5	0.88	272.06871	22.953	0.035
Chlorogenic acid	C16H18 O9	0.96	354.09542	19.149	0.033
Adenine	C5 H5 N5	1.07	135.05464	2.751	0.030

(*continued on next page*)

Table 2 (*continued*)

Name	Formula	Mass Deviation (ppm)	Molecular Weight (Da)	RT (min)	relative amount (%)
Calycosin	C16H12 O5	−1.09	284.06816	27.744	0.029
Aurantio-obtusin β-D-glucoside	C23H24 O12	1.53	492.12753	22.525	0.026
Medicarpin	C16H14 O4	0.95	270.08946	31.504	0.023
Dipotassium glycyrrhizinate	C42H60 O16	0.96	822.40511	26.368	0.021
Ginsenoside Rg2	C42H72 O13	1.44	830.50398	28.113	0.020
α-Linolenic acid	C18H30 O2	0.93	278.22484	40.115	0.017
Fraxetin	C10H8 O5	0.64	208.03731	20.432	0.017
Homoplantaginin	C22H22 O11	−0.56	462.11595	24.011	0.017
Cryptochlorogenic acid	C16H18 O9	0.93	354.09541	17.687	0.016
Alpinetin	C16H14 O4	0.83	270.08943	27.909	0.016
Daidzin	C21H20 O9	1.47	416.11134	21.272	0.016
p-Coumaric acid	C9 H8 O3	1.03	164.04751	21.327	0.016
Hispidulin	C16H12 O6	−0.29	300.0633	29.061	0.016
Iridin	C24H26 O13	1.47	522.13811	22.967	0.016
Chrysophanol 8-O-β-D-glucoside	C21H20 O9	0.88	416.1111	24.745	0.015
Diosmetin	C16H12 O6	−0.28	300.0633	28.134	0.014
Protocatechuic acid	C7 H6 O4	1	154.02676	19.504	0.014
Iristectorigenin B	C17H14 O7	0.9	330.07425	26.708	0.014
Salicylic acid	C7 H6 O3	0.64	138.03178	23.401	0.013
Naringenin chalcone	C15H12 O5	0.98	272.06874	27.223	0.013
Phellodendrine chloride	C20H24NO4.Cl	1.28	341.16304	19.595	0.010
Vicenin II	C27H30 O15	1.66	594.15945	19.779	0.010
Sibiricose A5	C22H30 O14	1.02	518.16408	19.886	0.009
Benzyl benzoate	C14H12 O2	1.28	212.084	25.517	0.009
Eriodictyol	C15H12 O6	0.57	288.06355	24.304	0.007
Complanatuside	C28H32 O16	1.35	624.16987	22.483	0.006
Diosmetin-7-O-β-D-glucopyranoside	C22H22 O11	1.28	462.1168	23.298	0.006

40.12 %, DL 0.75), and Jatrorrhizine (5.949 %; OB 30.44 %, DL 0.75). Palmatine (PLT) is a natural isoquinoline alkaloid that belongs to the class of protoberberines and exhibits anticancer activity in prostate cancer, breast cancer, colorectal adenocarcinoma and other cancers [26]. Numerous studies have shown that baicalin can exert anticancer activity through multiple pathways [27], while Jatrorrhizine can inhibit cancer cell proliferation and tumor growth and prevent metastasis through multiple mechanisms, and the important mechanism is to promote apoptosis of cancer cells [28]. Table 2 lists the chemical elements of BXD, and Fig. 1 displays the positive and negative ion chromatograms of BXD (Fig. 1A and B).

4.2. Cytotoxicity of BXD in vitro and its effect on TUC338 expression

qRT−PCR was used to determine the expression of TUC338 in gastric cancer tissues, paracarcinoma tissues, AGS human gastric cancer cells and GES-1 normal gastric mucosa cells and to detect the effects of BXD on the expression of TUC338 in AGS cells. We found that the expression of TUC.338 in gastric cancer tissues was higher than that in paracarcinoma tissues and that the expression of TUC338 in AGS was higher than that in GES-1 (Fig. 2A and B). The TUC338 RNA expression level in AGS cells was reduced by BXD (0.50, 1.00 and 1.50 mg/mL) in a concentration-dependent manner (Fig. 2C). MTT was used to detect the cytotoxicity of BXD on AGS cells. The findings demonstrate that BXD greatly suppressed the growth of AGS cells in a concentration-dependent manner. (Fig. 2D). The IC_{50} of BXD was 1.50 mg/mL for AGS cells. In the following study, we selected one noncytotoxic concentration (0.50 mg/mL), one low cytotoxic concentration (1.00 mg/mL), and half inhibitory concentration (1.50 mg/mL).

4.3. Inhibition of the migration and invasion of AGS cells by BXD

The effect of BXD on the invasion ability of AGS cells was examined by a cell scratch assay. The results showed that scratch wound healing was significantly slower in AGS cells treated with 1.00 and 1.50 mg/mL BXD, indicating that BXD had a concentration-dependent inhibitory effect on the migration of AGS cells (Fig. 3A and B). BXD significantly inhibited the migration and invasion of AGS cells in the Transwell assay in a concentration-dependent manner (Fig. 4A, B, C, D). The abilities of high concentrations of BXD and the positive control 5-FU to inhibit tumor cell invasion were essentially the same.

4.4. Lentiviral knockdown of TUC338

The expression level of lncRNA TUC338 in AGS cells transfected with TUC338 knockdown lentivirus was significantly reduced in comparison with that in cells transfected with TUC338-siRNA-ctrl (Fig. 5A and B).

4.5. Effects of reduced TUC338 expression on the migration and invasion of human gastric cancer AGS cells

The AGS cells with TUC338 knockdown had decreased invasion capability compared with the wild-type AGS cells (Fig. 6A and B).

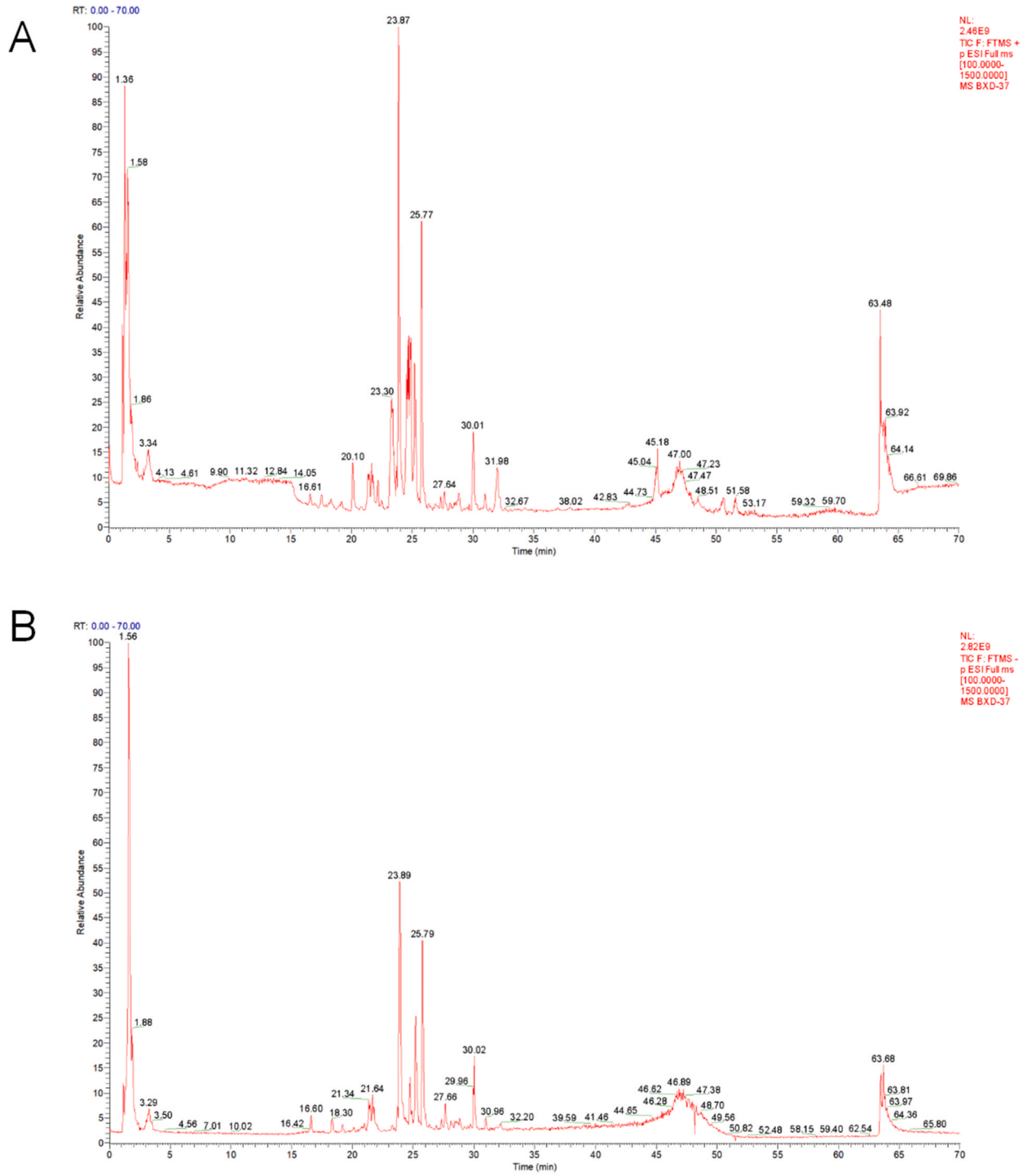

Fig. 1. TIC scan of BXD UHPLC–MS/MS chromatogram. (A) TIC scan of BXD UHPLC–MS/MS positive ion chromatogram. (B) TIC scan of BXD UHPLC–MS/MS negative ion chromatogram.

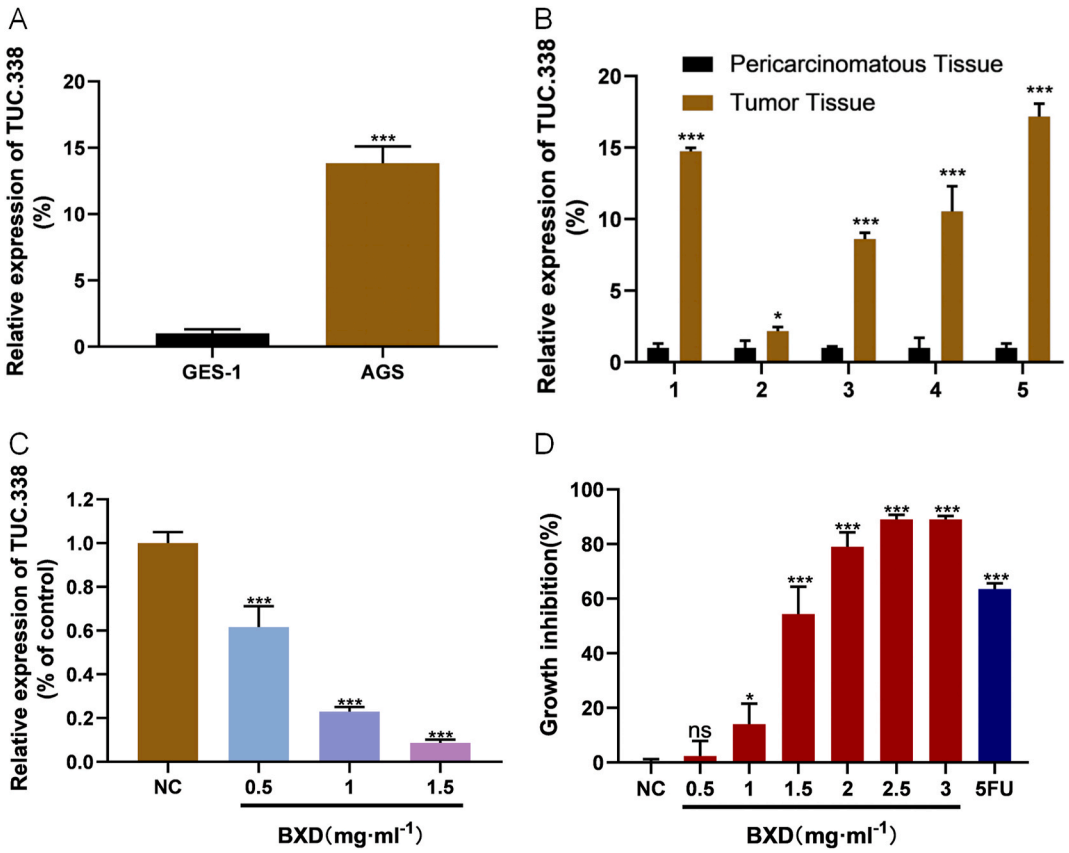

Fig. 2. *In vitro* cytotoxicity of BXD and its effect on TUC338 expression. (A) TUC338 expression in AGS cells was higher than that in GES-1 cells. (B) TUC338 expression in human gastric cancer was higher than that in paracarcinoma tissues. (C) TUC338 expression in AGS cells was decreased by BXD in a concentration-dependent manner. (D) BXD inhibited the growth of AGS cells in a concentration-dependent manner. One-way ANOVA: $*P < 0.05$ and $***P < 0.001$.

Compared to control AGS cells, AGS cells with TUC338 knockdown exhibited drastically inhibited migration (Fig. 6C and D).

4.6. *Effects of TUC338 knockdown on the expression levels of E-cadherin, N-cadherin and vimentin*

After TUC338 knockdown for 24 h, compared to the control AGS cells, E-cadherin protein expression was upregulated, whereas N-cadherin and vimentin protein levels were downregulated (Fig. 7A and B). After the knockdown of TUC338, compared to the control AGS cells, the RNA expression of E-cadherin rose, but N-cadherin and vimentin decreased (Fig. 7C).

4.7. *Quality control of BXD and the use of vitro experiments*

In vitro pharmacological studies have the advantages of rapidity, sensitivity, specificity, and easy-to-control conditions, which play an important role in the screening of drug activity, toxicity evaluation and in-depth research on cellular and molecular pharmacology. To ensure the quality control of the experimental drugs, we conducted three quality control tests on the BXD used in the present study using UHPLC–MS/MS. The comparison of positive ion and negative ion chromatograms of BXD is shown in Fig. 8 (Fig. 8A and B). Compound discover 3.2 software was used to extract the characteristic peaks of raw mass spectrum data from the three batches of BXD. Characteristic peaks were identified using the mzCloud online database and locally built mzVault database of natural products of traditional Chinese medicine. After manually confirming and eliminating repeated results, the chemical components screened remained basically unchanged. The main components, including palmatine (Long et al., 2019), berberine (Song et al., 2020) and baicalin (Singh S et al., 2021), have been found to possess anticancer effects. To explore whether BXD after decocting in traditional Chinese medicine has a special molecular pharmacological mechanism in human gastric cancer AGS cells, we adopted the method of directly treating the cells with the extract after processing BXD.

In addition, drug serum materials come from various physiological and pathological states of individuals, and there will be differences in drug-containing serum; moreover, after internal reactions, the drug content is further diluted, and the ingredients become more complex, increasing the difficulty of quality control. Additionally, some of the substances in the serum might be the metabolites

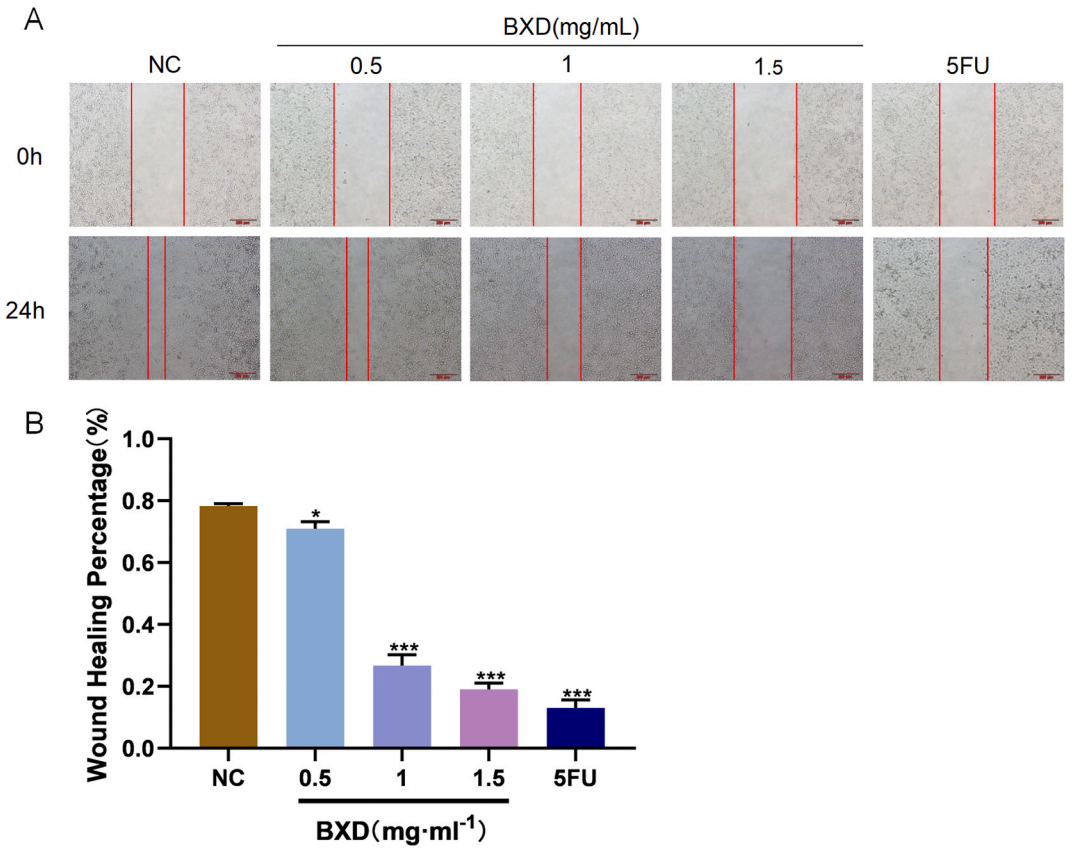

Fig. 3. Inhibition of AGS cell migration by BXD. (A) Scratch assay (Scale bar: 200 μm). (B) Graphical representation of the percentage of cell migration at 24 h. One-way ANOVA: $^{*}P < 0.05$ and $^{***}P < 0.001$.

of the drug. Therefore, if there is a feedback mechanism in the cells, the serum will act on the cells twice, which may conceal the actual effect of the drug serum. The drug-containing serum also interferes with the *in vitro* system, such as the influence of the serum itself on the enzyme activity *in vitro*. For the above reasons, we used *in vitro* administration.

5. Discussion

Gastric cancer has the second highest global incidence and mortality rate among oncologic diseases and is a major global public health threat [29]. According to the American Cancer Society, approximately 26,500 new cases of gastric cancer will be diagnosed in 2023 (15,930 in men and 10,570 in women), and 11,130 gastric cancer patients are expected to die in this year (6690 in men and 4400 in women) [30]. The prognosis of many oncological diseases has rapidly improved, but the 5-year survival rate of gastric cancer is approximately 20 %, which is still far from satisfactory [31]. Due to the lack of specific markers for identifying the early occurrence of gastric cancer and the fact that early symptoms of gastric cancer are not specific or even asymptomatic, many gastric cancers are diagnosed with distant metastases and directly lead to poor prognosis [32]. Meanwhile, due to the frequent occurrence of drug-resistant events and patients' intolerance to drugs, many gastric cancer patients eventually face a situation of being drug-free [33]. Therefore, there is an urgent need to find and develop new drugs for the clinical treatment of gastric cancer.

In both humans and mice, there are extremely conserved noncoding gene sequences, which we usually call ultraconserved regions (UCRs). Although UCRs themselves do not encode proteins, they can achieve phenotypic regulation of organisms by regulating mRNA expression and translation [33]. Subsequent studies revealed that some transcribed ultraconserved RNAs (TUCRs) play an important regulatory role in tumorigenesis and progression [34]. TUC338 was first identified as an oncogene that promotes an aggressive phenotype of colorectal cancer by targeting TIMP-1 [18]. Silencing TUC338 effectively inhibited the activation of the PI3K/AKT signaling pathway and, in doing so, suppressed tumor proliferation and migration [35], and subsequent studies suggested that this might be related to the regulation of miR-28–5p by TUC338 [36]. It has also been shown that TUC338 may promote tumor progression through upregulation of miR-10b, miR-466, and miR-1226–3p [17,37,38]. All these findings suggest that superconserved noncoding fragments such as TUC338 are still capable of performing transcription factor-like functions to accomplish the regulation of the malignant tumor phenotype; this is consistent with our results that downregulation of TUC338 expression resulted in a significant reduction in the invasive and migratory capacity of AGS cells and reversal of the EMT process compared to the null group. We found

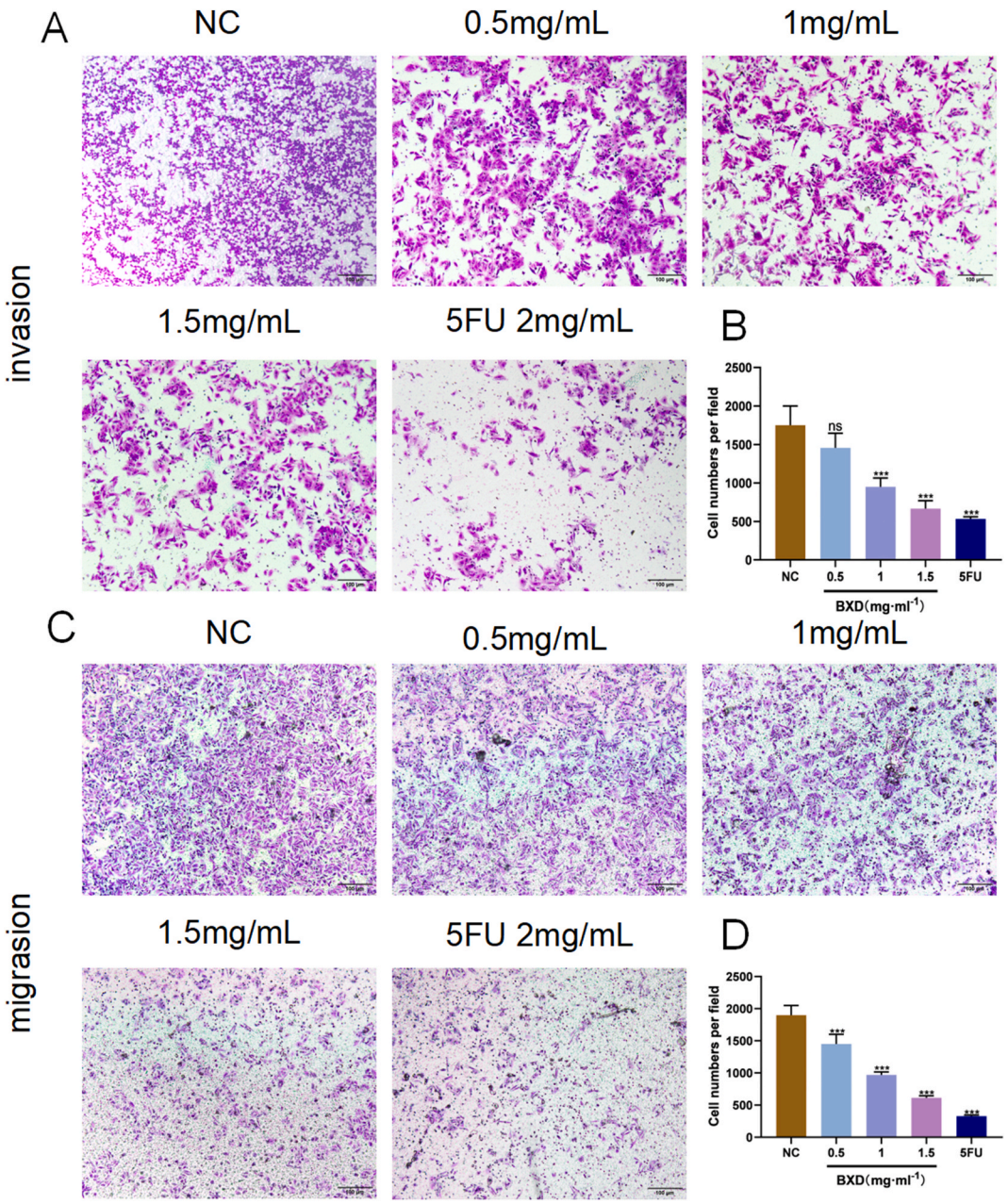

Fig. 4. Inhibition of the migration and invasion of AGS cells by BXD. (A) Transwell assay to analyze the effect of BXD on AGS cell invasion. (B) Graphical representation of cell invasion. (C) Transwell assay to analyze the effect of BXD on AGS cell migration. (D) Graphical representation of cell migration. One-way ANOVA: $***P < 0.001$.

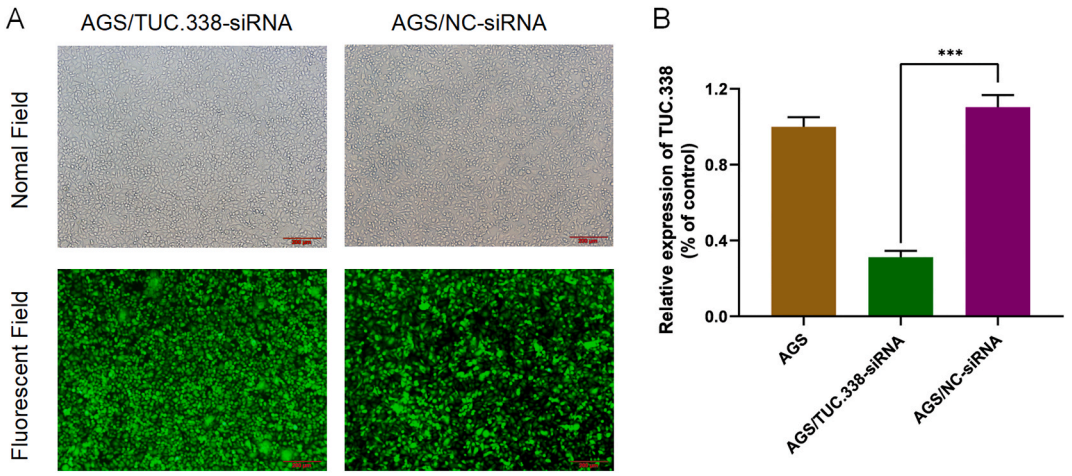

Fig. 5. The expression level of TUC338 in AGS cell lines and the establishment of TUC338 knockdown cell lines. (A) Fluorescence microscopy was used to photograph AGS cells after transfection. (B) The expression level of lncRNA TUC338 in AGS cells was significantly measured by qRT−PCR. One-way ANOVA: $***P < 0.001$.

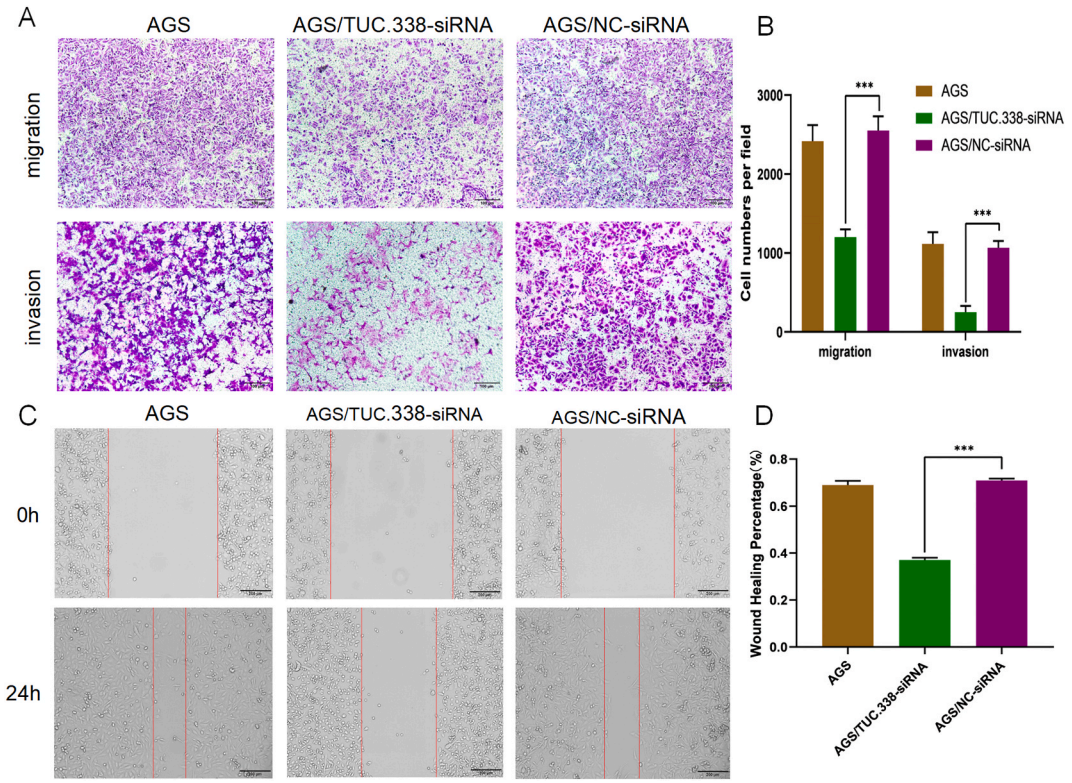

Fig. 6. Effects of reduced TUC338 expression on the migration and invasion of AGS cells. (A) Transwell assay to analyze AGS cell invasion and migration. (B) Graphical representation of cell invasion and migration. (C) Scratch assay to analyze AGS cell migration. (D) Graphical representation of cell migration. One-way ANOVA: $***P < 0.001$.

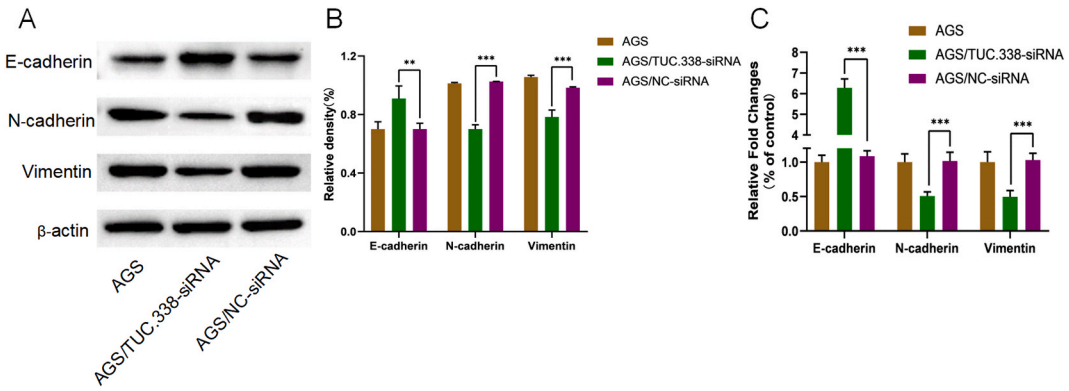

Fig. 7. Effects of TUC338 knockdown on the expression levels of E-cadherin, N-cadherin and vimentin. (A) Western blotting to analyze EMT-related proteins was altered by TUC338 knockdown. (B) E-cadherin protein expression was elevated, while N-cadherin and vimentin expression was decreased by TUC338 knockdown. (C) The EMT-related RNA level was measured by qPCR. E-cadherin RNA expression was elevated, and N-cadherin and vimentin RNA expression was decreased by TUC338 knockdown.

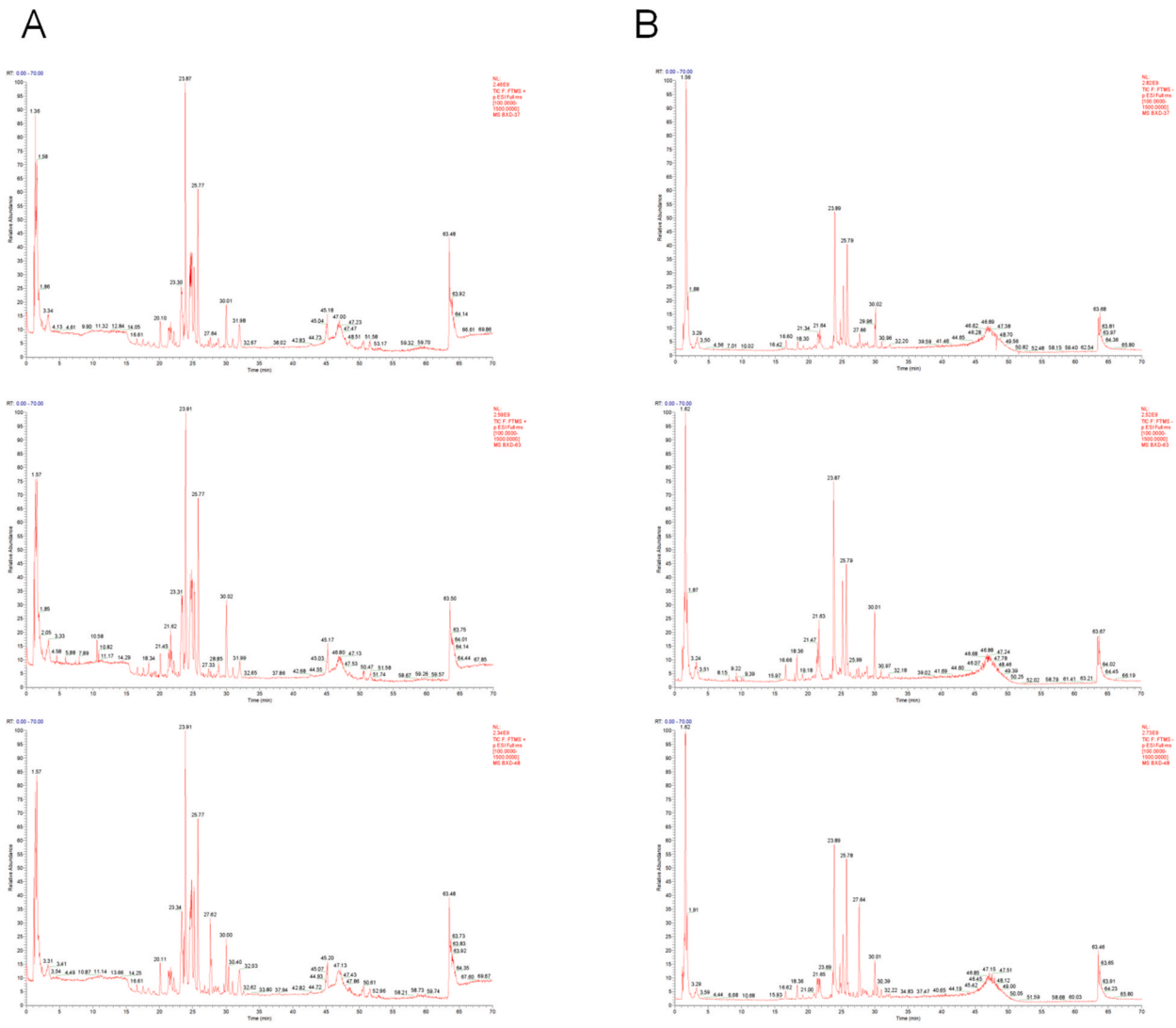

Fig. 8. Quality control of BXD. (A) TIC scan of BXD UHPLC–MS/MS positive ion chromatograms. (B) TIC scan of BXD UHPLC–MS/MS negative ion chromatograms.

that BXD dose-dependently downregulated TUC338 levels in AGS cells and downregulated the invasion and migration of gastric cancer cells. Therefore, we concluded that BXD is a potential TUC338 inhibitor with great promise for application in the clinical treatment of gastric cancer. However, there are some limitations in the present study. First, the current data have not been verified *in vivo*. Second, the specific mechanism by which TUC338 regulates EMT has not been elaborated. It is often difficult to identify the specific mechanism of compound regulation of biomolecules in the "black box" of traditional Chinese medicine prescriptions.

In conclusion, this study showed that BXD inhibited the invasive and migratory abilities of gastric cancer cells and was associated with the downregulation of TUC338. Our study reveals the theoretical basis of BXD for the treatment of gastric cancer and provides new evidence regarding the use of targeted noncoding RNAs for the treatment of malignant diseases.

Data availability statement

Data included in article/supp. material/referenced in article.

Additional information

No additional information is available for this paper.

CRediT authorship contribution statement

Xiaojun Dai: Supervision, Funding acquisition, Conceptualization. **Yanwei Yu:** Validation, Methodology, Investigation. **Chen Zou:** Writing – review & editing, Writing – original draft. **Bo Pan:** Visualization, Formal analysis. **Haibo Wang:** Supervision, Methodology, Formal analysis. **Shanshan Wang:** Writing – original draft, Formal analysis. **Xiaojuan Wang:** Visualization, Software. **Chenghai Wang:** Formal analysis. **Dongmei Liu:** Resources, Funding acquisition, Data curation. **Yanqing Liu:** Supervision, Resources, Methodology, Investigation, Funding acquisition, Conceptualization.

Declaration of competing interest

The authors declare that they have no known competing financial interests or personal relationships that could have appeared to influence the work reported in this paper.

Acknowledgments

We thank Dr Robert M. Hoffman (AntiCancer Inc., San Diego, CA, USA; Department of Surgery, University of California San Diego, CA, USA) for critical proofreading of this manuscript. This work was supported by National Natural Science Foundation of China (No. 81001589, No. 817739441); Special research project of business construction of national clinical research base of Traditional Chinese Medicine of State Administration of Traditional Chinese Medicine (No. JDZX2015254, No. JDZX2015091); Jiangsu Traditional Chinese Medicine science and technology project (No. YB201842); Top talent project funding of "six one project" for high level health talents in 2019 (LGY 2019031); Key R & D projects(Social Development) of Yangzhou in 2019 (yz2019065, yz2019064); The fifth and the sixth "333 programme" project; 2021 Natural Science Foundation of Nanjing University of Traditional Chinese Medicine (XZR2020097); The third batch of Jiangsu Province famous and old Chinese medicine experts inheritance studio construction project; Jiangsu Province Health Commission 2019 medical research project; The sixth batch of national traditional Chinese medicine experts' academic experience inheritance project; The second batch of Jiangsu Province TCM leading talent training target projects.

Appendix A. Supplementary data

Supplementary data to this article can be found online at https://doi.org/10.1016/j.heliyon.2023.e21064.

References

[1] A.P. Thrift, T.N. Wenker, H.B. El-Serag, Global burden of gastric cancer: epidemiological trends, risk factors, screening and prevention, Nat. Rev. Clin. Oncol. 20 (2023) 338–349.
[2] L. Yang, X. Ying, S. Liu, et al., Gastric cancer: epidemiology, risk factors and prevention strategies, Chin. J. Cancer Res. 32 (2020) 695–704.
[3] Z. Pelc, M. Skorzewska, K. Rawicz-Pruszynski, W.P. Polkowski, Lymph node involvement in advanced gastric cancer in the era of multimodal treatment-oncological and surgical perspective, Cancers 13 (2021) 2509.
[4] S. Chakraborty, K.B. Mir, N.D. Seligson, D. Nayak, R. Kumar, A. Goswami, Integration of EMT and cellular survival instincts in reprogramming of programmed cell death to anastasis, Cancer Metastasis Rev. 39 (2020) 553–566.
[5] W. Lu, Y. Kang, Epithelial-mesenchymal plasticity in cancer progression and metastasis, Dev. Cell 49 (2019) 361–374.
[6] M. Teeuwssen, R. Fodde, Wnt signaling in ovarian cancer stemness, EMT, and therapy resistance, J. Clin. Med. 8 (2019) 1658.
[7] M. Guttman, I. Amit, M. Garber, et al., Chromatin signature reveals over a thousand highly conserved large non-coding RNAs in mammals, Nature 458 (2009) 223–227.

[8] C.Y. Wang, D. Colognori, H. Sunwoo, D. Wang, J.T. Lee, PRC1 collaborates with SMCHD1 to fold the X-chromosome and spread Xist RNA between chromosome compartments, Nat. Commun. 10 (2019) 2950.
[9] M. Huang, H. Wang, X. Hu, X. Cao, lncRNA MALAT1 binds chromatin remodeling subunit BRG1 to epigenetically promote inflammation-related hepatocellular carcinoma progression, OncoImmunology 8 (2019), e1518628.
[10] B. Xiu, Y. Chi, L. Liu, et al., LINC02273 drives breast cancer metastasis by epigenetically increasing AGR2 transcription, Mol. Cancer 18 (2019) 187.
[11] W. Wang, W. Hu, Y. Wang, et al., Long non-coding RNA UCA1 promotes malignant phenotypes of renal cancer cells by modulating the miR-182-5p/DLL4 axis as a ceRNA, Mol. Cancer 19 (2020) 18.
[12] Z. Mao, Y. Wu, J. Zhou, C. Xing, Salinomycin reduces epithelial-mesenchymal transition-mediated multidrug resistance by modifying long noncoding RNA HOTTIP expression in gastric cancer cells, Anti Cancer Drugs 30 (2019) 892–899.
[13] Y. Han, J. Ye, D. Wu, et al., LEIGC long non-coding RNA acts as a tumor suppressor in gastric carcinoma by inhibiting the epithelial-to-mesenchymal transition, BMC Cancer 14 (2014) 932.
[14] J. Jia, D. Zhan, J. Li, Z. Li, H. Li, J. Qian, The contrary functions of lncRNA HOTAIR/miR-17-5p/PTEN axis and Shenqifuzheng injection on chemosensitivity of gastric cancer cells, J. Cell Mol. Med. 23 (2019) 656–669.
[15] G. Li, Y. Zhang, J. Mao, et al., lncRNA TUC338 is a potential diagnostic biomarker for bladder cancer, J. Cell. Biochem. 120 (2019) 18014–18019.
[16] T. Qian, H. Zhang, S. Yu, et al., Knockdown of lncRNA TUC338 inhibits esophageal cancer cells migration and invasion, J. Thorac. Dis. 13 (2021) 3061–3069.
[17] G. Li, Y. Zhang, J. Mao, et al., LncRNA TUC338 is overexpressed in prostate carcinoma and downregulates miR-466, Gene 707 (2019) 224–230.
[18] C. Wang, Z. Wang, J. Zhou, et al., 338 promotes invasion and metastasis in colorectal cancer, Int. J. Cancer 140 (2017) 1457–1464.
[19] B. Li, J. Rui, X. Ding, X. Yang, Exploring the multicomponent synergy mechanism of Banxia Xiexin Decoction on irritable bowel syndrome by a systems pharmacology strategy, J. Ethnopharmacol. 233 (2019) 158–168.
[20] W. Wang, C. Xu, X. Li, et al., Exploration of the potential mechanism of Banxia Xiexin Decoction for the effects on TNBS-induced ulcerative colitis rats with the assistance of network pharmacology analysis, J. Ethnopharmacol. 277 (2021), 114197.
[21] Y. Bai, Y. Chen, Y. Chen, et al., Efficacy of Banxia Xiexin decoction in a rat model of chronic atrophic gastritis, J. Tradit. Chin. Med. 39 (2019) 867–874.
[22] S. Yan, Y. Yue, J. Wang, et al., Banxia Xiexin decoction, a traditional Chinese medicine, alleviates colon cancer in nude mice, Ann. Transl. Med. 7 (2019) 375.
[23] Y. Yi, Z. Hu, R. Li, et al., Effectiveness of Banxia Xiexin Decoction in the treatment of precancerous lesions: a protocol for systematic review and meta-analysis, Medicine (Baltim.) 100 (2021), e25607.
[24] X. Sun, D. Xue, K. Zhang, F. Jiang, D. Li, Acrid-release and bitter-downbearing therapy and banxia xiexin decoction regulate Wnt/beta-catenin pathway, inhibit proliferation and invasion, and induce apoptosis in gastric cancer cells, Am J Transl Res. 13 (2021) 6211–6220.
[25] X. Feng, F. Xue, G. He, S. Huang, Q. Ni, Banxia xiexin decoction inhibits the expression of PD-L1 through multi-target and multi-pathway regulation of major oncogenes in gastric cancer, OncoTargets Ther. 14 (2021) 3297–3307.
[26] D. Tarabasz, Kukula-Koch W. Palmatine, A review of pharmacological properties and pharmacokinetics, Phytother Res. 34 (2020) 33–50.
[27] S. Singh, A. Meena, S. Luqman, Baicalin mediated regulation of key signaling pathways in cancer, Pharmacol. Res. 164 (2021), 105387.
[28] F. Zhong, Y. Chen, J. Chen, H. Liao, Y. Li, Y. Ma, Jatrorrhizine: a review of sources, pharmacology, pharmacokinetics and toxicity, Front. Pharmacol. 12 (2021), 783127.
[29] R.L. Siegel, K.D. Miller, H.E. Fuchs, A. Jemal, Cancer statistics, 2022, CA Cancer J. Clin. 72 (2022) 7–33.
[30] R.L. Siegel, K.D. Miller, N.S. Wagle, A. Jemal, Cancer statistics, 2023, CA Cancer J. Clin. 73 (2023) 17–48.
[31] E.C. Smyth, M. Nilsson, H.I. Grabsch, N.C. van Grieken, F. Lordick, Gastric cancer, Lancet 396 (2020) 635–648.
[32] N.Y. Chia, P. Tan, Molecular classification of gastric cancer, Ann. Oncol. 27 (2016) 763–769.
[33] T.H. Patel, M. Cecchini, Targeted therapies in advanced gastric cancer, Curr. Treat. Options Oncol. 21 (2020) 70.
[34] G.A. Calin, C.G. Liu, M. Ferracin, et al., Ultraconserved regions encoding ncRNAs are altered in human leukemias and carcinomas, Cancer Cell 12 (2007) 215–229.
[35] Z.W. Jia, Y. Li, X.Y. Kong, et al., Effects of long non-coding RNA-TUC338 on the migration and proliferation of lymphoma cells via PI3K/AKT signaling pathway, Zhongguo Shi Yan Xue Ye Xue Za Zhi 29 (2021) 494–499.
[36] Y. Li, Z. Jia, H. Zhao, et al., TUC338 promotes diffuse large B cell lymphoma growth via regulating EGFR/PI3K/AKT signaling pathway, J. Oncol. 2021 (2021), 5593720.
[37] G. Li, Y. Zhang, J. Mao, et al., lncRNA TUC338 is a potential diagnostic biomarker for bladder cancer, J. Cell. Biochem. 120 (2019) 18014–18019.
[38] J. Wang, L. Li, X. Jiang, et al., Silencing of long non-coding RNA TUC338 inhibits the malignant phenotype of nasopharyngeal cancer cells via modulating the miR-1226-3p/FGF2 axis, Discov Oncol. 13 (2022) 102.